Mapping Nodal Power Injections to Branch Flows in Connected LTI Electrical Networks

Yu Christine Chen, Abdullah Al-Digs
Department of Electrical and Computer Engineering
The University of British Columbia
Vancouver, BC V6T 1Z4
Email: {chen, aldigs}@ece.ubc.ca

Sairaj V. Dhople
Department of Electrical and Computer Engineering
University of Minnesota
Minneapolis, MN 55455
Email: sdhople@umn.edu

Abstract—This paper presents analytical closed-form expressions that map the contributions of nodal active- and reactive-power injections to the branch active- and reactive-power flows in an AC electrical network that is operating in sinusoidal steady state. We term these as the *power divider* laws, since they are derived leveraging, and their form and functionality are similar to, the ubiquitous current divider law. Distinct from the current divider law that only depends on the topology and constitution of the electrical network, the power divider laws are a function of the topology as well as the sinusoidal-steady-state voltage profile of the network.

I. INTRODUCTION

This paper derives analytical closed form expressions that map the active- and reactive-power injections in an AC electrical network operating in sinusoidal steady state to the active- and reactive-power flows on transmission lines in the network. In particular, we study connected electrical networks where lines are modelled as, and shunt elements are composed of, linear circuit components; and on some subset of nodes, we impose nonlinear active- and reactive-power injection constraints. This scenario captures the setting of the bulk AC power system with synchronous generators supplying constant-power loads through a linear time-invariant electrical network. (While we focus on AC networks, the DC counterpart, which follows as a straightforward extension, is applicable to networks of power-electronics converters.) The mapping from nodal current injections to line current flows in linear networks is linear, and commonly referred to as the current divider law. Since the expressions we derive essentially carry out the same function as the current divider law, but for complex-power injections and flows, we term them as the power divider laws. While the current divider law is linear, and only a function of the network topology, the power divider expressions are expectedly nonlinear, and depend on the network topology as well as the sinusoidal steady-state voltage profile of the network.

Numerous approaches have been applied to tackle the problem of mapping nodal power injections to branch flows in the literature. The major challenge in this task is that generators and loads in a power system are modelled as constant-power sources (CPSs) and loads (CPLs), respectively, which results in a nonlinear problem. Moreover, in general, branch active- and reactive-power flows are coupled to both nodal active- and reactive-power injections. Consequently, previous approaches in this domain are algorithmic or approximate in nature. Some relevant prior art includes: numerical approaches [1], [2], integration-based methods [3], utilizing current flows as proxies for power flows [4], and leveraging generation shift distribution factors [5], [6]. The method proposed in this paper is unique in that it offers an *analytical* approach to quantify the nonlinear relationship between branch power flows and nodal power injections. Furthermore, it tackles the *nonlinear* power-flow expressions and acknowledges injections from *all* buses in the network; no assumption is made about the existence or location of a slack bus that makes up for power imbalances.

Beginning with an existing power flow solution, we examine the algebraic power-balance expressions in a compact matrix-vector form to derive the mapping between branch power flows and nodal power injections. The derivation and eventual power divider expressions leverage information from the current divider laws. In their original form, the power divider expressions are a function of the voltage phasors at *all* the nodes in the network. However, leveraging Kron reduction—a circuit reduction procedure that preserves the electrical terminal behaviour in a set of predefined boundary nodes—we demonstrate that only the voltage phasors at the nodes with nonzero external current injections are required to recover the flows on all the lines.

The most obvious application of these expressions would be in the fair usage allocation of transmission lines in an AC power system network. However, given the prevalent competitive electricity environment, outlining the fraction of a transmission-line (branch) flow uniquely to each generator/load (at a node) is potentially useful in a variety of settings to ensure that electricity markets can be designed in a fair and efficient manner. In this regard, we also envision applications to transmission network expansion, transmission network loss allocation, real-time visualization, and spot pricing. Steering clear from power-systems-specific applications, in this paper, we illustrate ideas by focusing on a four-node star network with three nodes having constant-power constraints. In so doing, we illustrate how the power divider laws can extract the contributions of injections to the flows on all branches in this network while only requiring the voltages at the three nodes with constant-power injections.

II. NETWORK DESCRIPTION

Consider an AC electrical network operating in steady-state with N nodes, collected in the set $\mathcal{N}$. The set of branches is represented by $\mathcal{E} := \{(m,n)\} \subseteq \mathcal{N} \times \mathcal{N}$. Each branch is modelled using the lumped-parameter Π-model with series admittance $y_{mn} \in \mathbb{C}$ and shunt admittance $y_{mn}^{\text{sh}} \in \mathbb{C}$. Then, the entries of the the network admittance matrix, denoted by $Y_{\mathcal{N}}$, are[1]

$$[Y_{\mathcal{N}}]_{mn} := \begin{cases} y_m + \sum_{(m,k)\in\mathcal{E}} y_{mk}, & \text{if } m = n, \\ -y_{mn}, & \text{if } (m,n) \in \mathcal{E}, \\ 0, & \text{otherwise}, \end{cases} \quad (1)$$

where

$$y_m = g_m + \mathrm{j}b_m := y_{mm} + \sum_{k\in\mathcal{N}_m} y_{mk}^{\text{sh}}, \quad (2)$$

denotes the total shunt admittance connected to node m with $\mathcal{N}_m \subseteq \mathcal{N}$ representing the set of neighbours of node m and $y_{mm} \in \mathbb{C}$ any passive shunt elements connected to node m.

Denote the set of B boundary nodes in the electrical circuit as $\mathcal{B} \subseteq \mathcal{N}$, and similarly denote the set of interior nodes as $\mathcal{I} = \mathcal{N} \setminus \mathcal{B}$. Furthermore, collect steady-state nodal voltages of boundary and interior nodes as $V = [V_1, \ldots, V_B]^{\text{T}}$ and $V_{\mathcal{I}} = [V_{B+1}, \ldots, V_N]^{\text{T}}$, respectively, where $V_i = |V_i|\angle\theta_i$ represents the voltage phasor at node i. Also let $I = [I_1, \ldots, I_B]^{\text{T}}$ and $I_{\mathcal{I}} = [I_{B+1}, \ldots, I_N]^{\text{T}}$ represent the vectors of current injections into boundary and interior nodes, respectively, where I_i denotes the phasor of the current injected into node i. Then, application of Kirchhoff's current law at each node yields

$$\begin{bmatrix} I \\ I_{\mathcal{I}} \end{bmatrix} = \begin{bmatrix} Y_{\mathcal{BB}} & Y_{\mathcal{BI}} \\ Y_{\mathcal{BI}}^{\text{T}} & Y_{\mathcal{II}} \end{bmatrix} \begin{bmatrix} V \\ V_{\mathcal{I}} \end{bmatrix}. \quad (3)$$

Since the interior nodes are only connected to passive LTI circuit elements, the entries of $I_{\mathcal{I}}$ are equal to zero in (3). Assuming that the submatrix $Y_{\mathcal{II}}$ is nonsingular, then the second set of equations in (5) can be uniquely solved to obtain the interior nodal voltages as

$$V_{\mathcal{I}} = -Y_{\mathcal{II}}^{-1}Y_{\mathcal{BI}}^{\text{T}}V. \quad (4)$$

Substituting this back into the first set of equations in (3), we obtain

$$I = \left(Y_{\mathcal{BB}} - Y_{\mathcal{BI}}Y_{\mathcal{II}}^{-1}Y_{\mathcal{BI}}^{\text{T}}\right) V =: YV. \quad (5)$$

This model reduction through a *Schur complement* of the admittance matrix is known as *Kron reduction* [7]. We refer to the matrix Y in (3) as the *Kron-reduced admittance matrix*. As an example, the circuit in Fig. 1a reduces to the one in Fig. 1b through this process. We remark that, even though the Kron-reduced admittance matrix Y is well-defined, it is not necessarily the admittance matrix of a passive circuit.

Finally, denote the vector of nodal complex-power injections into boundary nodes by $S = [S_1, \ldots, S_B]^{\text{T}} = P + \mathrm{j}Q$, with $P = [P_1, \ldots, P_B]^{\text{T}}$ and $Q = [Q_1, \ldots, Q_B]^{\text{T}}$. Then,

---

[1]$[Y_{\mathcal{N}}]_{mn}$ denotes the entry in the m-th row and n-th column of the matrix $Y_{\mathcal{N}}$.
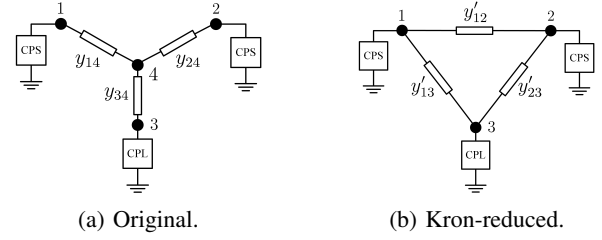

(a) Original.   (b) Kron-reduced.

Fig. 1: Original and Kron-reduced circuits.

nodal complex-power injections into boundary nodes can be expressed as

$$S = \text{diag}\,(V)\,I^*, \quad (6)$$

where $\text{diag}\,(V)$ denotes a diagonal matrix formed with entries of the vector V.

III. NETWORK BRANCH FLOWS

In this section, we delineate how nodal current injections map to branch current flows, from which an exact mapping from nodal complex-power injection to branch complex-power flows is developed.

A. Branch Current Flows

Via notation introduced in Section II, the current flow in branch $(m,n) \in \mathcal{E}$, from node m to n, can be expressed as

$$I_{(m,n)} = y_{mn}(V_m - V_n) + y_{mn}^{\text{sh}}V_m$$
$$= \left(y_{mn}e_{mn}^{\text{T}} + y_{mn}^{\text{sh}}e_m^{\text{T}}\right) \begin{bmatrix} V \\ V_{\mathcal{I}} \end{bmatrix}, \quad (7)$$

where $e_m \in \mathbb{R}^N$ denotes a column vector of all zeros except with the m-th entry equal to 1, and $e_{mn} := e_m - e_n$. Substitution of (4) into the above yields

$$I_{(m,n)} = \left(y_{mn}e_{mn}^{\text{T}} + y_{mn}^{\text{sh}}e_m^{\text{T}}\right) \begin{bmatrix} V \\ -Y_{\mathcal{II}}^{-1}Y_{\mathcal{BI}}^{\text{T}}V \end{bmatrix}$$
$$= \left(y_{mn}e_{mn}^{\text{T}} + y_{mn}^{\text{sh}}e_m^{\text{T}}\right) \begin{bmatrix} \text{diag}(\mathbb{1}_B) \\ -Y_{\mathcal{II}}^{-1}Y_{\mathcal{BI}}^{\text{T}} \end{bmatrix} V$$
$$= \left(y_{mn}e_{mn}^{\text{T}} + y_{mn}^{\text{sh}}e_m^{\text{T}}\right) \begin{bmatrix} \text{diag}(\mathbb{1}_B) \\ -Y_{\mathcal{II}}^{-1}Y_{\mathcal{BI}}^{\text{T}} \end{bmatrix} Y^{-1}I \quad (8)$$

where the third equality above results from substituting $V = Y^{-1}I$ in (5) and $\mathbb{1}_B$ denotes the $B \times 1$ vector with all ones. Subsequently, (8) can be expressed as $I_{(m,n)} = \kappa_{(m,n)}^{\text{T}}I$, where $\kappa_{(m,n)} \in \mathbb{C}^B$ is given by

$$\kappa_{(m,n)}^{\text{T}} = \left(y_{mn}e_{mn}^{\text{T}} + y_{mn}^{\text{sh}}e_m^{\text{T}}\right) \begin{bmatrix} \text{diag}(\mathbb{1}_B) \\ -Y_{\mathcal{II}}^{-1}Y_{\mathcal{BI}}^{\text{T}} \end{bmatrix} Y^{-1}. \quad (9)$$

The entries of $\kappa_{(m,n)}$ correspond to the current injection sensitivity factors of branch (m,n) with respect to the current injection at node $i \in \mathcal{B}$. Note that the expression in (7) is a generalization of the *current divider* law, which typically applies to the particular case of a single current source feeding a set of impedances connected in parallel [8].

B. Branch Complex-power Flows

Denote, by $S_{(m,n)} = P_{(m,n)} + jQ_{(m,n)}$, the complex-power flow in branch (m,n), which can be expressed as

$$S_{(m,n)} = V_m I^*_{(m,n)}, \tag{10}$$

where

$$V_m = e_m^{\mathrm{T}} \begin{bmatrix} V \\ V_{\mathcal{I}} \end{bmatrix} = e_m^{\mathrm{T}} \begin{bmatrix} V \\ -Y_{\mathcal{II}}^{-1} Y_{\mathcal{BI}}^{\mathrm{T}} V \end{bmatrix} = e_m^{\mathrm{T}} \begin{bmatrix} \mathrm{diag}(\mathbb{1}_B) \\ -Y_{\mathcal{II}}^{-1} Y_{\mathcal{BI}}^{\mathrm{T}} \end{bmatrix} V.$$

Substitution of current injection sensitivity factors from (9) into (10) yields

$$S_{(m,n)} = V_m \left(\kappa_{(m,n)}^{\mathrm{T}} \right)^* I^*. \tag{11}$$

Furthermore, by eliminating I^* from (11) using (6), we obtain

$$S_{(m,n)} = V_m \left(\kappa_{(m,n)}^{\mathrm{T}} \right)^* \left(\mathrm{diag}\,(V) \right)^{-1} S, \tag{12}$$

which exactly relates steady-state complex-power flow in branch (m,n) in the original full circuit as a function of nodal voltage phasors and complex-power nodal injections of the Kron-reduced circuit. Using the phasor form of nodal voltages, (12) is rewritten as[2]

$$
\begin{aligned}
S_{(m,n)} &= \left(|V_m| e^{j\theta_m} \right) \left(\kappa_{(m,n)}^{\mathrm{T}} \right)^* \mathrm{diag}\left(\frac{\mathbb{1}_B}{|V| \circ \exp(j\theta)} \right) S \\
&= |V_m| \left(\kappa_{(m,n)}^{\mathrm{T}} \right)^* \mathrm{diag}\left(\frac{\mathbb{1}_B e^{j\theta_m}}{|V| \circ \exp(j\theta)} \right) S \\
&= |V_m| \left(\kappa_{(m,n)}^{\mathrm{T}} \right)^* \mathrm{diag}\left(\frac{\exp(j\theta^m)}{|V|} \right) S, \tag{13}
\end{aligned}
$$

where the third equality above results by defining $\theta^m := \theta_m \mathbb{1}_B - \theta$. In order to uncover mappings between branch power flows and nodal power injections from (13), decompose the current injection sensitivity factors from (9) into real and imaginary components as

$$\kappa_{(m,n)} = \alpha_{(m,n)} + j\beta_{(m,n)}.$$

Leveraging the above decomposition and separating real and imaginary components of (13), we obtain

$$P_{(m,n)} = \mathrm{Re}\{S_{(m,n)}\} = |V_m| \left(u_{(m,n)}^{\mathrm{T}} P - v_{(m,n)}^{\mathrm{T}} Q \right), \tag{14}$$

$$Q_{(m,n)} = \mathrm{Im}\{S_{(m,n)}\} = |V_m| \left(u_{(m,n)}^{\mathrm{T}} Q + v_{(m,n)}^{\mathrm{T}} P \right), \tag{15}$$

where $u_{(m,n)}, v_{(m,n)} \in \mathbb{R}^B$ are given by

$$u_{(m,n)} = \mathrm{diag}\left(\frac{\cos \theta^m}{|V|} \right) \alpha_{(m,n)} + \mathrm{diag}\left(\frac{\sin \theta^m}{|V|} \right) \beta_{(m,n)}, \tag{16}$$

$$v_{(m,n)} = \mathrm{diag}\left(\frac{\sin \theta^m}{|V|} \right) \alpha_{(m,n)} - \mathrm{diag}\left(\frac{\cos \theta^m}{|V|} \right) \beta_{(m,n)}. \tag{17}$$

Note that (14)–(15) are nonlinear functions that are linearly related to active- and reactive-power nodal injections P and Q, while nonlinearities involving $|V|$ and θ appear in the multiplicative factors $u_{(m,n)}$ and $v_{(m,n)}$.

[2]$\mathrm{diag}(x/y)$ forms a diagonal matrix with the m-th entry given by x_m/y_m, where x_m and y_m are the m-th entries of vectors x and y, respectively. $x \circ y$ denotes entry-wise product of vectors x and y.

C. Attributing Nodal Injections to Branch Flows

The expressions in (14) and (15) reveal the contribution of each nodal injection to the net active- and reactive-power flows in branch (m,n). To see this, note that (14) and (15) can be expressed as the additive sum of $2B$ scalar terms, each of which is linear in the nodal active- and reactive-power injections at node i, as follows:

$$P_{(m,n)} = |V_m| \left(\sum_{i=1}^{B} e_i^{\mathrm{T}} u_{(m,n)} P_i - \sum_{i=1}^{B} e_i^{\mathrm{T}} v_{(m,n)} Q_i \right), \tag{18}$$

$$Q_{(m,n)} = |V_m| \left(\sum_{i=1}^{B} e_i^{\mathrm{T}} u_{(m,n)} Q_i + \sum_{i=1}^{B} e_i^{\mathrm{T}} v_{(m,n)} P_i \right). \tag{19}$$

Apparent from (18)–(19) is that the active- and reactive-power branch flows are coupled to both active- and reactive-power nodal injections. Consequently, in order to extract the contribution of node i to active- and reactive-power branch flows, denoted by $P_{(m,n),i}$ and $Q_{(m,n),i}$, respectively, the nodal active- and reactive-power injection contributions are combined as follows:

$$P_{(m,n),i} = |V_m| e_i^{\mathrm{T}} \left(u_{(m,n)} P_i - v_{(m,n)} Q_i \right), \tag{20}$$

$$Q_{(m,n),i} = |V_m| e_i^{\mathrm{T}} \left(u_{(m,n)} P_i + v_{(m,n)} Q_i \right). \tag{21}$$

Here, it is worth noting that $P_{(m,n),i}$ and $Q_{(m,n),i}$ are scalar quantities that, in general, can be either positive or negative (or zero). We interpret this observation from a branch flow direction perspective. Specifically, positive $P_{(m,n),i}$ and $Q_{(m,n),i}$ denote bus i's contribution to branch (m,n) active- and reactive-power flow, respectively, in the forward direction. On the other hand, negative $P_{(m,n),i}$ and $Q_{(m,n),i}$ contribute to branch (m,n) active- and reactive-power flows in the reverse direction.

IV. CASE STUDIES

Consider the 4-node AC electric circuit with the one-line diagram shown in Fig. 1a. In this circuit, constant-power sources (CPSs) are connected to nodes 1 and 2, injecting $P_1 = 0.75$ p.u. and $P_2 = 0.25$ p.u., respectively. A constant-power load (CPL) is connected to node 3, with active-power injection $P_3 = -1$ p.u. and reactive-power injection $Q_3 = -0.5$ p.u. The voltage magnitudes at nodes 1 and 2 are regulated at $|V_1| = 1$ p.u. and $|V_2| = 1$ p.u., respectively. Branches are modelled using lumped parameters, where $y_{14} = -j10$ p.u. with $y_{14}^{\mathrm{sh}} = j0.005$ p.u., $y_{24} = -j15$ p.u., $y_{34} = -j10$ p.u. Using the parameters listed above, we compute the power flow solution that consists of all nodal voltages. Then, Kron reduction allows us to compute nodal injection contributions to branch active- and reactive-power flows using only boundary node voltages (specifically nodes 1, 2, and 3), in conjunction with (20) and (21).

1) Three-branch Case: Results with respect to active-power flows in branches $(1,4)$, $(2,4)$, and $(4,3)$ are reported in Table I, rows 1–3, respectively. Column 6 reports the branch net active-power flow. Columns 3–5 show the nodal injection contributions to the branch active-power flows from boundary

TABLE I: Nodal injection contributions to branch active-power flows. All quantities are in p.u.

| | Line (m,n) | Nodal Contributions $P_{(m,n),i}$ | | | $P_{(m,n)}$ |
		$i=1$	$i=2$	$i=3$	
Three-branch Case	$(1,4)$	0.75	0	0	0.75
	$(2,4)$	0	0.25	0	0.25
	$(4,3)$	0	0	1	1
Four-branch Case	$(1,2)$	0.141	-0.105	0.186	0.221
	$(1,4)$	0.609	0.105	-0.186	0.529
	$(2,4)$	0.142	0.141	0.189	0.471
	$(4,3)$	0	0	1	1

nodes 1–3, respectively. All contributions are positive in value, indicating each $P_{(m,n),i}$ contributes to the forward-direction flow in each branch. Node 1 injection contributes 0.75 p.u. to the active-power flow in branch $(1,4)$, node 2 injection contributes 0.25 p.u. to that in branch $(2,4)$, and node 3 contributes 1 p.u. to branch $(4,3)$. Nodal injection contributions from nodes 1, 2, and 3 represent 100% of the active-power flow in branches $(1,4)$, $(2,4)$, and $(4,3)$, respectively. These contributions are visually depicted in Fig. 2.

2) Four-branch Case: In addition to the aforementioned branches, we add a fourth branch $(1,2)$ to the network in Fig. 1a, which is modelled with a series admittance $y_{12} = -j10$ p.u. Numerical values for branches $(1,2)$, $(1,4)$, $(2,4)$, and $(4,3)$ are reported in Table I, rows 4–7, respectively. The additional branch reveals nodal injection contributions to both forward- and reverse-direction flows in branches $(1,2)$ and $(1,4)$, as indicated by positive- and negative-valued quantities, respectively. In Fig. 3, forward-direction (F) and reverse-direction (R) flows are grouped accordingly. Superimposed over each branch are pie charts that describe the percentage contribution of a specific boundary node towards the total forward-direction and reverse-direction branch active-power flow. Note that $P_{(m,n),i}$ obtained from (20) is a scalar quantity that, in general, only contributes to the forward-direction or reverse-direction flow (or neither). Interestingly, Fig. 3 reveals a loop flow of 0.186 p.u. in the loop that consists of branches $(1,2)$, $(2,4)$, and $(4,1)$, due to the injection at node 3.

V. CONCLUDING REMARKS

In this paper, we derive and examine the mapping between branch active- and reactive-power flows and nodal power injections. Leveraging Kron reduction, we demonstrate that the flows on all branches can be recovered from only nodal voltages at boundary nodes. We focus on branch active-power flows and visualize the corresponding mapping via pie charts superimposed onto the one-line diagram of a canonical four-node star network. Compelling avenues for future work are to leverage the mapping for applications such as spot pricing, transmission-services pricing, and real-time visualization.

REFERENCES

[1] D. Kirschen, R. Allan, and G. Strbac, "Contributions of individual generators to loads and flows," *IEEE Transactions on Power Systems*, vol. 12, no. 1, pp. 52–60, February 1997.
[2] J. Bialek, "Allocation of transmission supplementary charge to real and reactive loads," *IEEE Transactions on Power Systems*, vol. 13, no. 3, pp. 749–754, August 1998.
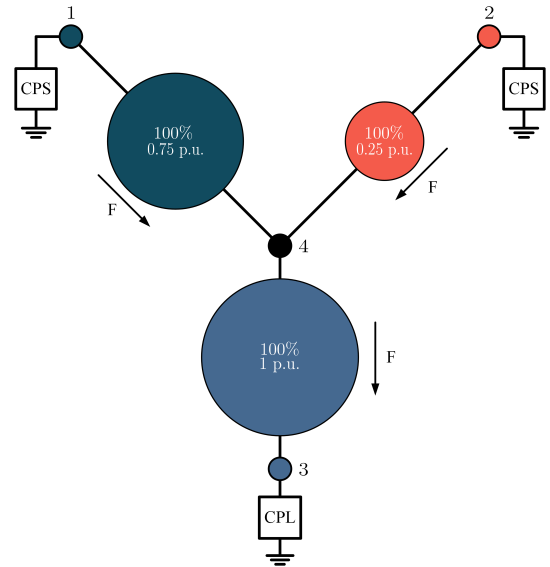
Fig. 2: Three-branch case: nodal injection contributions to branch active-power flows.
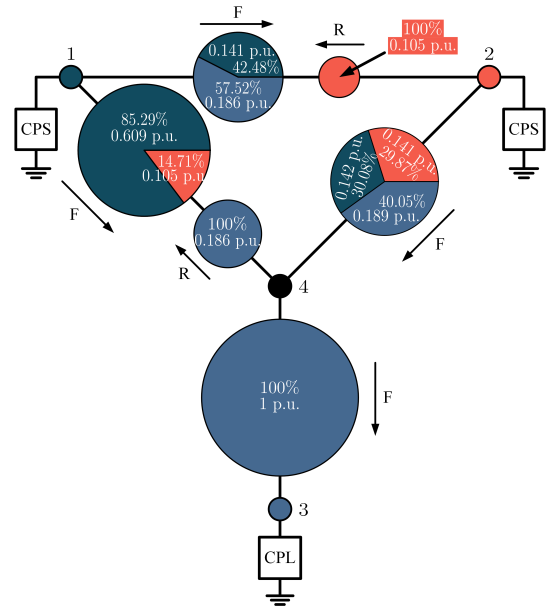

Fig. 3: Four-branch case: nodal injection contributions to branch active-power flows.

[3] A. Fradi, S. Brignone, and B. F. Wollenberg, "Calculation of energy transaction allocation factors," *IEEE Transactions on Power Systems*, vol. 16, no. 2, pp. 266–272, May 2001.
[4] A. J. Conejo, J. Contreras, D. A. Lima, and A. Padilha-Feltrin, "Zbus transmission network cost allocation," *IEEE Transactions on Power Systems*, vol. 22, no. 1, pp. 342–349, February 2007.
[5] H. Rudnick, R. Palma, and J. Fernandez, "Marginal pricing and supplement cost allocation in transmission open access," *IEEE Transactions on Power Systems*, vol. 10, no. 2, pp. 1125–1132, May 1995.
[6] A. M. L. da Silva, J. G. de Carvalho Costa, and L. H. Lopes Lima, "A new methodology for cost allocation of transmission systems in interconnected energy markets," *IEEE Transactions on Power Systems*, vol. 28, no. 2, pp. 740–748, May 2013.
[7] R. A. Horn and C. R. Johnson, *Matrix Analysis*. New York, NY: Cambridge University Press, 2013.
[8] A. S. Sedra and K. C. Smith, *Microelectronic Circuits Revised Edition*, 5th ed. New York, NY, USA: Oxford University Press, Inc., 2007.